

Mott-Hubbard Metal-Insulator Transition in Paramagnetic V_2O_3 : An LDA+DMFT(QMC) Study

K. Held,^{1,*} G. Keller,¹ V. Eyert,¹ D. Vollhardt,¹ and V.I. Anisimov²

¹*Institut für Physik, Universität Augsburg, 86135 Augsburg, Germany*

²*Institute of Metal Physics, Ekaterinburg GSP-170, Russia*

(Received 1 December 2000)

The electronic properties of paramagnetic V_2O_3 are investigated by the computational scheme LDA+DMFT(QMC). This approach merges the local density approximation (LDA) with dynamical mean-field theory (DMFT) and uses quantum Monte Carlo simulations (QMC) to solve the effective Anderson impurity model of DMFT. Starting with the crystal structure of metallic V_2O_3 and insulating $(V_{0.962}Cr_{0.038})_2O_3$ we find a Mott-Hubbard transition at a Coulomb interaction $U \approx 5$ eV. The calculated spectrum is in very good agreement with experiment. Furthermore, the orbital occupation and the spin state $S = 1$ determined by us agree with recent polarization dependent x-ray-absorption experiments.

DOI: 10.1103/PhysRevLett.86.5345

PACS numbers: 71.27.+a, 74.25.Jb, 79.60.-i

The metal-insulator transition within the paramagnetic phase of V_2O_3 is generally considered to be the classical example of a Mott-Hubbard metal-insulator transition (MIT) [1]. During the last few years, our understanding of the MIT in the one-band Hubbard model has considerably improved, in particular due to the application of dynamical mean-field theory (DMFT).

Within DMFT the electronic lattice problem is mapped onto a self-consistent single-impurity Anderson model. The mapping becomes exact in the limit of infinite coordination number [2] and allows one to investigate the dynamics of correlated lattice electrons nonperturbatively at all interaction strengths. This is of essential importance for a problem such as the MIT which occurs at a Coulomb interaction comparable to the electronic bandwidth. The transition is signaled by the collapse of the quasiparticle peak at the Fermi energy when the interaction is increased [3]. Rozenberg *et al.* [4] first applied DMFT to investigate the metal-insulator transition in V_2O_3 in terms of the one-band Hubbard model. Subsequently, the influence of orbital degeneracy was studied by means of the two- [5–7] and three-band [6] Hubbard model for the semielliptic density of states (DOS) of a Bethe lattice.

Clearly, a realistic theory of V_2O_3 must take into account the complicated electronic structure of this system. In the high-temperature paramagnetic phase V_2O_3 has a corundum crystal structure in which the V ions are surrounded by an octahedron of oxygen ions. This leads to an electronic structure with a $3d^2V^{3+}$ state, where the two e_g orbitals are empty and the three t_{2g} orbitals are filled with two electrons. A small trigonal distortion lifts the triple degeneracy of the t_{2g} orbitals, resulting in one nondegenerate a_{1g} orbital oriented along the c axis and two degenerate e_g^π orbitals oriented predominantly in the hexagonal plane. Starting from this orbital structure Castellani *et al.* [8] proposed a widely accepted model with a strong covalent a_{1g} bond between two V ions along the c axis. This bonding state is occupied by a singlet pair (one electron per V) and hence does not contribute to

the local magnetic moment. The remaining electron per V has a twofold orbital degeneracy within the e_g^π orbitals and a spin $S = 1/2$. This $S = 1/2$ model suggested that the half-filled, one-band Hubbard model was the simplest possible electronic model describing V_2O_3 . However, recent experimental results by Park *et al.* [9] obtained by polarized x-ray spectroscopy seem to require an interpretation in terms of a $S = 1$ spin state, and an $e_g^\pi e_g^\pi$ orbital state with an admixture of $e_g^\pi a_{1g}$ configurations. Subsequently, Ezhov *et al.* [10] and Mila *et al.* [11] argued for $S = 1$ models without and with orbital degeneracy, respectively, for the antiferromagnetic insulating phase of V_2O_3 . LDA+ U calculations indicate that the atomic Hund's rule is responsible for the high-spin ground state of the V ions [10]. While LDA+ U may be used to describe the antiferromagnetic insulating phase of V_2O_3 , the metal-insulator transition within the correlated *paramagnetic* phase is beyond the scope of this approach since the Coulomb interaction is treated within Hartree-Fock. Here the computational scheme LDA+DMFT [12–15], obtained by combining electronic band structure theory (LDA) with the many-body technique DMFT [2], is the best available method for the investigation of real systems close to a Mott-Hubbard MIT [16]. To solve the DMFT equations we employ quantum Monte Carlo simulations (QMC) which yield a numerically exact solution [17]; the resulting calculational scheme is referred to as LDA+DMFT(QMC) [13,15,16].

We start by calculating the density of states (DOS) of paramagnetic *metallic* V_2O_3 and paramagnetic *insulating* $(V_{0.962}Cr_{0.038})_2O_3$, respectively, within LDA using the crystal structure data of Dernier [18,19]. In the LDA DOS, Fig. 1, one observes the expected behavior: the V t_{2g} states are near the Fermi energy and are split into a nondegenerate a_{1g} band and doubly degenerate e_g^π bands; the V e_g^σ states are at higher energies. The results for corundum V_2O_3 and $(V_{0.962}Cr_{0.038})_2O_3$ are very similar, and are close to those found by Mattheiss [20] and Ezhov *et al.* [10] for the corundum and the monoclinic phase.

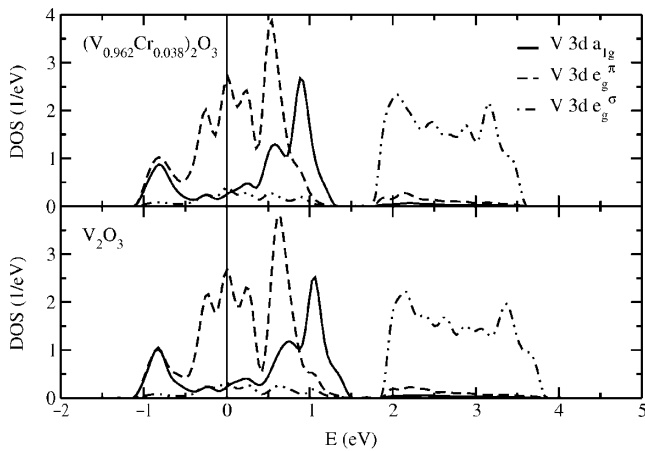


FIG. 1. Partial DOS of the 3d bands for paramagnetic metallic V_2O_3 and insulating $(V_{0.962}Cr_{0.038})_2O_3$.

Going from metallic V_2O_3 to insulating $(V_{0.962}Cr_{0.038})_2O_3$ the metal-metal distances are increased, in particular, in the crystallographic c direction. This results in a slight narrowing of the t_{2g} and e_g^σ bands by ≈ 0.2 and 0.1 eV, respectively, as well as a weak down-shift of the centers of gravity of both groups of bands. Most important is the fact that the insulating gap observed experimentally for the Cr-doped system is *missing* in the LDA DOS. It is generally believed that this insulating gap is due to strong Coulomb interactions which cannot be described adequately within LDA. Using LDA+DMFT(QMC) we will now show explicitly that the insulating gap is indeed caused by the electronic correlations.

In the LDA+DMFT approach [12–16] the LDA band structure, expressed by a one-particle Hamiltonian H_{LDA}^0 , is supplemented with the local Coulomb repulsion U and Hund's rule exchange J :

$$\hat{H} = \hat{H}_{LDA}^0 + U \sum_{im} \hat{n}_{m\uparrow}^i \hat{n}_{m\downarrow}^i + \sum_{im \neq \tilde{m}\sigma\tilde{\sigma}} (V - \delta_{\sigma\tilde{\sigma}} J) \hat{n}_{m\sigma}^i \hat{n}_{\tilde{m}\tilde{\sigma}}^i. \quad (1)$$

Here, i denotes the lattice site; m and \tilde{m} enumerate the three interacting t_{2g} orbitals. The interaction parameters are related by $V = U - 2J$ which holds exactly for degenerate orbitals and is a good approximation for the t_{2g} orbitals which are almost degenerate. Furthermore, since the t_{2g} bands at the Fermi energy are rather well separated from all other bands we restrict the calculation to these bands (for details of the computational scheme, see Refs. [15,16]). With this restriction and by taking into account the lattice symmetry which leads to vanishing off-diagonal matrix elements between the t_{2g} orbitals, one can show that only the LDA DOS of the three t_{2g} bands shown in Fig. 1 enter the LDA+DMFT calculation [16]. While the Hund's rule coupling J is insensitive to screening effects and may thus be obtained within LDA to a good accuracy ($J = 0.93$ eV [21]), the LDA-calculated value of the Coulomb repulsion U has a typical uncertainty of at

least 0.5 eV [15]. For this reason, we adjust U to yield a metal-insulator transition with Cr doping. *A posteriori*, we compare whether the adjusted value is in the range of what is to be expected from a constraint LDA calculation and whether other experimental properties such as the photo-emission spectrum are in agreement with our calculation.

The spectra obtained by LDA+DMFT(QMC) are shown in Fig. 2 [22]. They imply that the critical value of U for the MIT is about 5 eV. Indeed, at $U = 4.5$ eV one observes pronounced quasiparticle peaks at the Fermi energy, i.e., characteristic metallic behavior, even for the crystal structure of $(V_{0.962}Cr_{0.038})_2O_3$, while at $U = 5.5$ eV the form of the calculated spectral function is typical for an insulator for both sets of crystal structure parameters. At $U = 5.0$ eV one is then at, or very close to, the MIT since there is a pronounced dip in the DOS at the Fermi energy for both a_{1g} and e_g^π orbitals for the crystal structure of $(V_{0.962}Cr_{0.038})_2O_3$, while for pure V_2O_3 one still finds quasiparticle peaks. (We note that at $T \approx 0.1$ eV one observes only metallic-like and insulator-like behavior, with a rapid but smooth crossover between these two phases, since a sharp MIT occurs only at lower temperatures [3,5]). The critical value of the Coulomb interaction $U \approx 5$ eV is in reasonable agreement with the values determined spectroscopically by fitting to model calculations, and by constrained LDA. The former gives $U = 4-5$ eV for vanadium oxides [23] while the latter yields [21] $U \approx 3$ eV (for $LaVO_3$) to $U \approx 8$ eV, depending on whether the e_g electrons participate in the screening or not; without screening, one finds $U \approx 6-7$ eV [24].

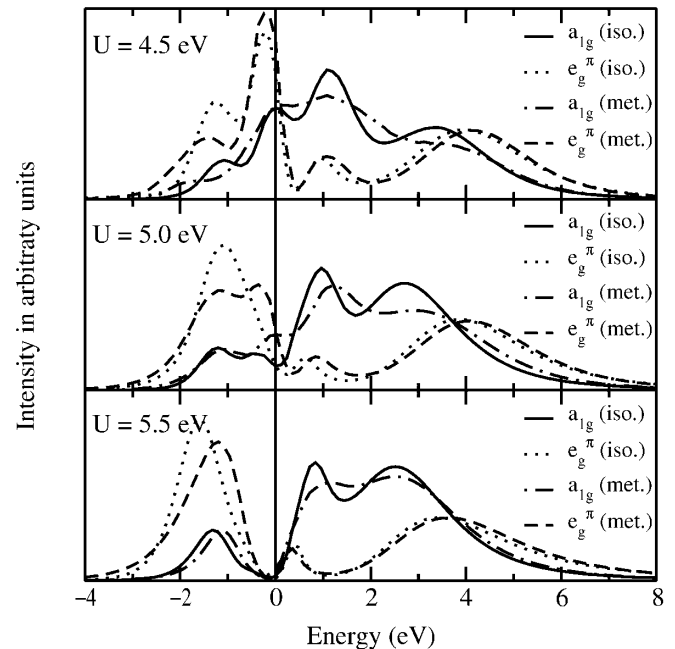


FIG. 2. LDA+DMFT(QMC) spectra for paramagnetic $(V_{0.962}Cr_{0.038})_2O_3$ ("iso.") and V_2O_3 ("met.") at $U = 4.5, 5,$ and 5.5 eV, and $T = 0.1$ eV ≈ 1000 K.

To compare with the photoemission spectrum of V_2O_3 by Schramme *et al.* [25], the LDA+DMFT(QMC) spectra of Fig. 2 are multiplied with the Fermi function at $T = 0.1$ eV and Gauss broadened by 0.05 eV to account for the experimental resolution. The theoretical results for $U = 5$ eV are seen to be in good agreement with experiment (Fig. 3), in contrast with the LDA results. We also note that the DOS is highly asymmetric with respect to the Fermi energy due to the orbital degrees of freedom. The comparison between our results, the data of Müller *et al.* [26] obtained by x-ray absorption measurements, and LDA in Fig. 4 shows that, in contrast with LDA, our results not only describe the different bandwidths above and below the Fermi energy (≈ 6 eV and $\approx 2-3$ eV, respectively) correctly, but even resolve the two-peak structure above the Fermi energy. Also the interpretation of the two peaks is different in LDA and LDA+DMFT(QMC). While in the latter approach the peak at lower energies (1 eV) has predominantly a_{1g} character and the peak at higher energy (3 eV) is due to the e_g^π Hubbard bands (see Fig. 2), in LDA the a_{1g} and e_g^π states contribute only below 1.8 eV such that the second peak is entirely due to the e_g^σ states (see Fig. 1).

Particularly interesting are the spin and the orbital degrees of freedom in V_2O_3 . We find (not shown) that for $U \geq 3$ eV the squared local magnetic moment $\langle m_z^2 \rangle = \langle (\sum_m [\hat{n}_{m\uparrow} - \hat{n}_{m\downarrow}])^2 \rangle$ saturates at a value of 4, i.e., there are *two* electrons with the same spin direction in the $(a_{1g}, e_{g1}^\pi, e_{g2}^\pi)$ orbitals. Thus, we conclude that the spin state of V_2O_3 is $S = 1$ throughout the Mott-Hubbard transition region. Note, that at $U = J = 0$ only the lower maximum of the a_{1g} band is filled with both spin species (Fig. 1). This a_{1g} singlet corresponds to the filled a_{1g}

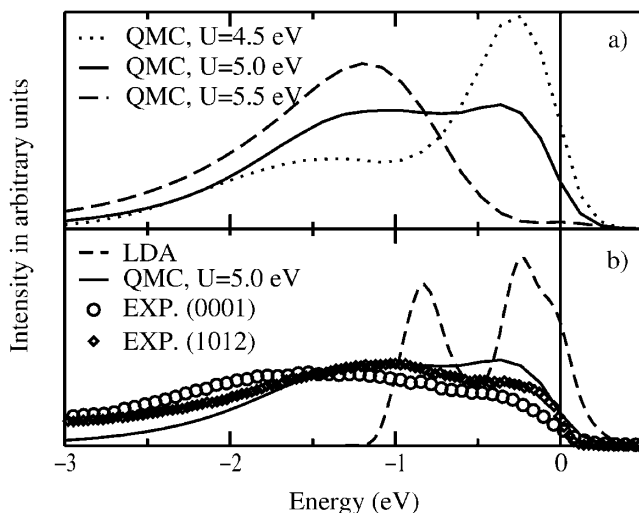


FIG. 3. (a) LDA+DMFT(QMC) spectrum for $U = 4.5, 5,$ and 5.5 eV at $T = 0.1$ eV ≈ 1000 K; (b) comparison with the LDA spectrum and the photoemission experiment by Schramme *et al.* [25] for two different V_2O_3 single-crystal surfaces at $T = 300$ K. Note that the $(10\bar{1}2)$ surface has the same coordination number as the bulk.

binding orbital in the Castellani *et al.* $S = 1/2$ model. However, it is destroyed with increasing U and J as the system tries to avoid double occupations and unaligned spins, respectively. Our $S = 1$ result agrees with the measurements of Park *et al.* [9] and also with the data for the high-temperature susceptibility [27]. The latter correspond to an effective magnetic moment $\mu_{\text{eff}} = 2.66\mu_B$ which is close to the ideal value $\mu_{\text{eff}} = 2.83\mu_B$ for $S = 1$. The result is at odds with a $S = 1/2$ model and with the results for a one-band Hubbard model where m_z^2 changes substantially at the MIT [3].

For the orbital degrees of freedom we find a predominant occupation of the e_g^π orbitals, but with a significant admixture of a_{1g} orbitals. This admixture decreases at the MIT: in the metallic phase we determine the occupation of the $(a_{1g}, e_{g1}^\pi, e_{g2}^\pi)$ orbitals as $(0.37, 0.815, 0.815)$, and in the insulating phase as $(0.28, 0.86, 0.86)$. This should be compared with the experimental results of Park *et al.* [9]. From their analysis of the linear dichroism data the authors concluded that the ratio of the configurations $e_g^\pi e_g^\pi : e_g^\pi a_{1g}$ is equal to 1:1 for the paramagnetic metallic and 3:2 for the paramagnetic insulating phase, corresponding to a one-electron occupation of $(0.5, 0.75, 0.75)$ and $(0.4, 0.8, 0.8)$, respectively. Although our results show a somewhat smaller value for the admixture of a_{1g} orbitals, the overall behavior, including the tendency of a *decrease* of the a_{1g} admixture across the transition to the insulating state, are well reproduced. This agrees with the LDA+ U calculation for the antiferromagnetic insulating phase [10]. Further experimental evidence for predominant (e_g^π, e_g^π) configurations was obtained by polarized neutron diffraction by Brown *et al.* [28]. Measuring the spatial distribution of the magnetization induced by a magnetic field, they showed that the moment induced on the V atoms is almost entirely due to the electrons in the e_g^π orbitals. Note that this orbital occupation and the spectral distribution of Fig. 2 are due to DOS effects, i.e., differences in the centers of gravity and bandwidths of the e_g^π

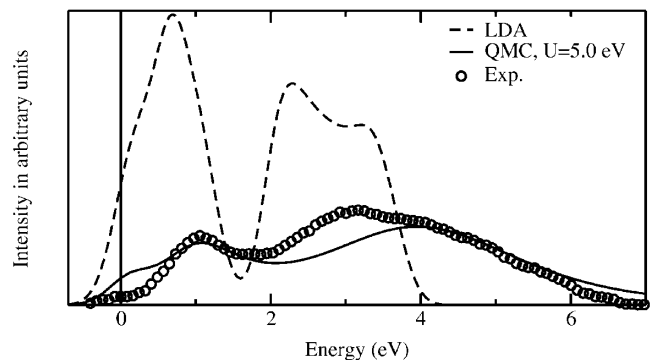


FIG. 4. Comparison of the LDA and LDA+DMFT(QMC) spectra at $T = 0.1$ eV (Gaussian broadened with 0.2 eV) with the x-ray absorption data of Müller *et al.* [26]. The LDA and QMC curves are normalized differently since the e_g^σ states, which are shifted towards higher energies if the Coulomb interaction is included, are neglected in our calculation.

and a_{1g} bands as well as the band-edge maxima of the a_{1g} band (Fig. 1). The latter are due to a bonding-antibonding splitting.

In conclusion, starting from the LDA-calculated spectra for paramagnetic V_2O_3 and $(V_{0.962}Cr_{0.038})_2O_3$, and including the missing electronic correlations via DMFT(QMC), we showed that a Mott-Hubbard MIT occurs in the paramagnetic phase at $U \approx 5$ eV. Our results are in very good agreement with the experimentally determined photoemission and x-ray absorption spectra, i.e., above and below the Fermi energy. Furthermore, we calculate the spin state to be $S = 1$ and find an orbital admixture of $e_g^\pi e_g^\pi$ and $e_g^\pi a_{1g}$ configurations, which both agree with recent experiments. Thus LDA+DMFT(QMC) provides a remarkably accurate microscopic theory of the strongly correlated electrons in the paramagnetic phase of V_2O_3 .

The MIT will eventually become first order at lower temperatures [3,4]; QMC simulations at $T \approx 300$ K are under way, but are very computer expensive. Furthermore, future investigations will have to clarify the origin of the discontinuous lattice distortion at the first-order MIT which leaves the lattice symmetry unchanged. Here various scenarios are possible [29,30]. In particular, the MIT might be the driving force behind the lattice distortion by causing a thermodynamic instability with respect to changes of the lattice volume and distortions.

We acknowledge valuable discussions with J. W. Allen, N. Blümer, R. Claessen, U. Eckern, K.-H. Höck, S. Horn, H.-D. Kim, and S. A. Sawatzky. We thank A. Sandvik for making available his maximum entropy code. This work was supported by the DFG through SFB 484 and Forschergruppe HO 955/2, by the Russian Foundation for Basic Research Grant No. RFFI-01-02-17063, by the John v. Neumann-Institut für Computing, Jülich, and by the Alexander von Humboldt-Foundation (K. H.).

*Present address: Physics Department, Princeton University, Princeton, NJ 08544.

Electronic address: kheld@feynman.princeton.edu

- [1] N.F. Mott, *Rev. Mod. Phys.* **40**, 677 (1968); *Metal-Insulator Transitions* (Taylor & Francis, London, 1990); F. Gebhard, *The Mott Metal-Insulator Transition* (Springer, Berlin, 1997).
- [2] W. Metzner and D. Vollhardt, *Phys. Rev. Lett.* **62**, 324 (1989); A. Georges *et al.*, *Rev. Mod. Phys.* **68**, 13 (1996).
- [3] G. Moeller *et al.*, *Phys. Rev. Lett.* **74**, 2082 (1995); J. Schlipf *et al.*, *Phys. Rev. Lett.* **82**, 4890 (1999); M.J. Rozenberg, R. Chitra, and G. Kotliar, *Phys. Rev. Lett.* **83**, 3498 (1999); R. Bulla, *Phys. Rev. Lett.* **83**, 136 (1999).
- [4] M.J. Rozenberg *et al.*, *Phys. Rev. Lett.* **75**, 105 (1995).
- [5] M.J. Rozenberg, *Phys. Rev. B* **55**, R4855 (1997).
- [6] J.E. Han, M. Jarrell, and D.L. Cox, *Phys. Rev. B* **58**, R4199 (1998).
- [7] K. Held and D. Vollhardt, *Eur. Phys. J. B* **5**, 473 (1998).
- [8] C. Castellani, C. R. Natoli, and J. Ranninger, *Phys. Rev. B* **18**, 4945 (1978); **18**, 4967 (1978); **18**, 5001 (1978).
- [9] J.-H. Park *et al.*, *Phys. Rev. B* **61**, 11 506 (2000).
- [10] S. Yu. Ezhov *et al.*, *Phys. Rev. Lett.* **83**, 4136 (1999).
- [11] F. Mila *et al.*, *Phys. Rev. Lett.* **85**, 1714 (2000).
- [12] V.I. Anisimov *et al.*, *J. Phys. Condens. Matter* **9**, 7359 (1997).
- [13] A. I. Lichtenstein and M. I. Katsnelson, *Phys. Rev. B* **57**, 6884 (1998).
- [14] M. B. Zöfl *et al.*, *Phys. Rev. B* **61**, 12 810 (2000).
- [15] I. A. Nekrasov *et al.*, *Eur. Phys. J. B* **18**, 55 (2000).
- [16] For an introduction into LDA+DMFT, see K. Held *et al.*, cond-mat/0010395.
- [17] For a comparison of LDA+DMFT results for the photoemission spectra of $La_{1-x}Sr_xTiO_3$ obtained by different numerical techniques, see Ref. [15].
- [18] P.D. Dernier, *J. Phys. Chem. Solids* **31**, 2569 (1970).
- [19] Use of the crystal structure of Cr-doped V_2O_3 for the insulating phase of pure V_2O_3 is justified by the observation that Cr doping is equivalent to the application of (negative) pressure.
- [20] L. F. Mattheiss, *J. Phys. Condens. Matter* **6**, 6477 (1994).
- [21] I. Solovyev, N. Hamada, and K. Terakura, *Phys. Rev. B* **53**, 7158 (1996).
- [22] All QMC results presented were obtained for $T = 0.1$ eV. Simulations for V_2O_3 at $U = 5$ eV, $T = 0.143$ eV, and $T = 0.067$ eV suggest, however, only a minor smoothing of the spectrum with increasing temperature.
- [23] A. T. Mizokawa and A. Fujimori, *Phys. Rev. B* **48**, 14 150 (1993); J. Zaanen and G. A. Sawatzky, *J. Solid State Chem.* **88**, 8 (1990).
- [24] V.I. Anisimov, J. Zaanen, and O.K. Andersen, *Phys. Rev. B* **44**, 943 (1991); V.I. Anisimov, F. Aryasetiawan, and A. I. Lichtenstein, *J. Phys. Condens. Matter* **9**, 767 (1997).
- [25] M. Schramme, Ph.D. thesis, Universität Augsburg, 2000; M. Schramme *et al.* (unpublished). Recent experiments at higher photon energies by H.-D. Kim *et al.* (unpublished) show an even better agreement.
- [26] O. Müller *et al.*, *Phys. Rev. B* **56**, 15 056 (1997).
- [27] D.J. Arnold and R.W. Mires, *J. Chem. Phys.* **48**, 2231 (1968).
- [28] P.J. Brown, M. M. R. Costa, and K. R. A. Ziebeck, *J. Phys. Condens. Matter* **10**, 9581 (1998).
- [29] P. Majumdar and H. R. Krishnamurthy, *Phys. Rev. Lett.* **73**, 1525 (1994).
- [30] J. W. Allen and R. M. Martin, *Phys. Rev. Lett.* **49**, 1106 (1982); M. Lavagna, C. Lacroix, and M. Cyrot, *J. Phys. F* **13**, 1007 (1983); C. Huscroft, A. K. McMahan, and R. T. Scalettar, *Phys. Rev. Lett.* **82**, 2342 (1999); K. Held *et al.*, *Phys. Rev. Lett.* **85**, 373 (2000).